Atmospheric Research 151 (2015) 250–258

Contents lists available at ScienceDirect

Atmospheric Research

journal homepage: www.elsevier.com/locate/atmos

Mechanical characteristics of Raschel mesh and their application to the design of large fog collectors

Juan de Dios Rivera *, Diego Lopez-Garcia

Centro del Desierto de Atacama/School of Engineering, Pontificia Universidad Catolica de Chile, Av. Vicuña Mackenna 4860, Macul, Santiago RM 782-0436, Chile

ARTICLE INFO

Article history:
Received 1 November 2013
Received in revised form 5 May 2014
Accepted 24 June 2014
Available online 30 June 2014

Keywords:
Large fog collector
Fog
Raschel mesh
Tensile test
Wind force

ABSTRACT

Fog collection can alleviate water scarcity in certain arid regions of the World. However, large fog collectors frequently fail under the load of strong wind events. This is mainly due to lack of engineered design and the absence of data on mechanical properties of the meshes used as collecting surface. Indeed, engineering methods permit to design a structure to withstand any desired wind speed. In this study we obtained the mechanical properties of a particular Raschel mesh, the most commonly used material for fog collection, by means of tensile tests. We found that Raschel mesh is very anisotropic, having a stiff and elastic behavior in the knitting, or longitudinal direction, whereas in the transverse direction has an extremely flexible (virtually no stiffness), nonlinear behavior. Using a relatively simple 2-D structural model, we show that the maximum wind pressure a mesh can withstand is inversely proportional to the distance between the sides of the frame that supports the mesh. As a consequence, we recommend installing this mesh with the longitudinal direction aligned with the shortest dimension of the mesh-holding frame, if maximum strength and minimum deformation are desired. The structural model also indicates that the mesh can withstand very strong winds, over 50 m/s assuming a steady wind velocity for the typical large fog collectors as presently installed. Possible reasons why the mesh has been observed to break at weaker winds are then discussed.

1. Introduction

Fog collection can alleviate water scarcity problems in certain arid areas. It has been studied and proved for decades as a feasible alternative source of fresh water in arid areas with the presence of suitable persistent fog (Klemm et al., 2012; Lummerich and Tiedemann, 2011; Schemenauer and Cereceda, 1991, 1994; Schemenauer et al., 1988). This fog is common in arid and semi-arid areas close to the ocean, where clouds are formed over the sea and then pushed by predominant winds towards the continent, where they turn into fog when intercepted by high lands. This kind of fog is addressed as 'Advection fog', although sometimes orographic fog also contributes to fog water collection (Cereceda et al., 2002, 2008b). Several studies have recognized the potential of fog collection for human consumption around the world, in places such as: Pacific coast of central South America (Cereceda et al., 2008a, 2008b, 2002; Larrain et al., 2002; de la Lastra, 2002), the Canary Islands (Marzol, 2002, 2008), Morocco (Marzol and Sánchez, 2008), South Africa (Olivier, 2002; Olivier and de Rautenbach, 2002; Louw et al., 1998), Oman (Abdul-Wahab and Lea, 2008; Abdul-Wahab et al., 2010), Saudi Arabia (Al-hassan, 2009; Gandhidasan and Abualhamayel, 2007), western Mediterranean basin (Estrela et al., 2008), and Namibia (Shanyengana et al., 2002).

Since the first studies made by Carlos Espinosa in Chile (Gishler, 1991), fog collection projects had relied on different designs of fog collection devices, where the flat screen Large Fog Collector (LFC, see Fig. 1) is the most common type of design used in the last decades (Schemenauer et al., 1988; Schemenauer and Cereceda, 1994; Gischler, 1991). The

* Corresponding author. Tel.: +56 2 2354 5886; fax: +56 2 2354 5828.
E-mail address: jrivera@ing.puc.cl (J.D. Rivera).

http://dx.doi.org/10.1016/j.atmosres.2014.06.011
0169-8095/

Fig. 1. Failure of large fog collectors: (top; Peña Blanca, Chile) failure of the supporting structure; (bottom, left; Anagua project — Canary Island, with permit by Carlos Sanchez Recio) failure of the foundation; (bottom, right; Peña Blanca, Chile) breakage of the mesh.

materials used for the LFC are usually simple components, locally available, because the main focus of fog collection projects has been to provide fresh water to small, poor communities around the world. These projects have been mainly supported by non-governmental organizations (NGO), which are responsible to install the system (Klemm et al., 2012; Schemenauer et al., 2005).

One of the main problems that affects the sustainability of fog collection projects is the maintenance of LFCs that are frequently damaged by strong winds events, the sun (UV radiation) and other environmental factors which affect the structure, mesh and other components (Schemenauer et al., 2005). Indeed, when subjected to extreme wind loads (the only relevant load on LFCs), many LFCs fail and/or lose functionality. Some representative examples can be seen in Fig. 1. In some cases, LFCs collapse because of failure of the supporting structure (Fig. 1, top), whereas in some other cases they collapse because of failure of the foundation (Fig. 1, bottom left). Finally, in most other cases LFCs lose functionality because the mesh breaks and hence loses its ability to collect water (Fig. 1, bottom right).

Recently, Klemm at al. (2012) made a thorough review of existing LFC installations around the world. However, they did not analyze in detail the effects of wind pressure on the mesh and the supporting structure, and the effect of design variables on water collection efficiency. Indeed, it is noteworthy that, as far as we know, no peer review publication has dealt with the currently observed mesh breakage or structural collapse of LFCs caused by extreme winds.

The reason why LFCs exhibit such a poor reliability is undoubtedly the lack of a rational (i.e., “engineered”) design process. In other words, most existing LFCs are non-engineered structures. Thus, the implementation of structural engineering principles is then clearly necessary in order to extend the life cycle of LFCs and, consequently, to make them more cost-effective. In this regard, it is interesting to note that, although various geometric layouts have been proposed and implemented, the load path in LFCs is always the same: wind imposes pressures on the mesh, which in turn impose forces on the supporting structure, and these forces are ultimately transferred to the foundation. If the load is known, forces on the mesh and on the supporting structure can be easily calculated through the

application of standard structural engineering methods and, once these forces are known, the supporting structure can be easily designed to withstand such forces. However, the assessment of forces on the mesh and on the supporting structures requires knowledge of their mechanical properties. In the case of the supporting structure, these properties are usually known because its members (e.g., beams, columns, cables) have many other structural engineering applications and, hence, have been already characterized, in some cases in detail. The properties of the mesh, on the other hand, are largely unknown: they have not been characterized mainly because typical mesh materials of LFCs do not have structural applications.

There are two main design types of LFCs, one type uses rigid frames to hold the mesh and the other uses a flexible frame made with cables. It has been observed that the rigid frame design is more prone to damage by strong winds than the flexible frame one, because the latter bends and adopts a shape that better supports wind forces. The ONG FogQuest has been quite successful in installing flexible frame LFCs all over the world with relatively long useful life. This is the result of a good design and a sound building practice.

The objective of this paper is to characterize, qualitatively and quantitatively, the mechanical properties of the Raschel mesh, which is by far the most used mesh material in LFCs (Klemm et al., 2012). Such properties are then considered in the engineered design of rectangular LFCs, and some practical design recommendations are then proposed.

2. Material and methods

The Raschel mesh tested in this study corresponds to the standard, black, polyethylene mesh produced in Chile by Marienberg,[1] with 35% shade coefficient and treated for UV-resistance. The knitting pattern of this mesh produces a significant anisotropy of its mechanical properties. Indeed, along the knitting (longitudinal) direction, there are continuous filaments, which are apparent in Fig. 2, whereas in the transverse direction, the filaments are not continuous and are knotted to the longitudinal ones. Therefore, it is expected that there will be much more elongation in the transverse direction than in the longitudinal direction under the application of the same force. Additionally, when transversely stretching the mesh, the longitudinal filaments will deform perpendicularly to their axis, direction for which every filament has almost no resistance, and the knots of the transverse filaments onto the longitudinal ones will tighten. These two effects combined lead to a significant permanent deformation resulting in a large elongation in the transverse direction and contraction in the longitudinal one.

For characterizing the mechanical properties relevant for the structural design of Raschel mesh in both directions, we performed several tensile tests to selected specimens. All tensile tests were performed at the Laboratory of Metallurgy of the Mechanical and Metallurgical Engineering Department, Pontificia Universidad Catolica de Chile, according to ASTM Standard D4595-11. This standard was developed for geo-textiles, but we could not find a specific standard for Raschel mesh and we believe that this is probably the most appropriate standard for characterizing this material. Following the recommendations of this standard, we made special clamps to hold the specimen on the tensile test machine, as depicted in Figs. 3 and 4. The dimensions of the specimen, length L and width w, were kept constant for all tests. Especial care had to be taken while mounting the specimen in the clamps, to avoid slipping of the mesh off the clamps during the test. Best results were obtained gluing the mesh to the clamps' wedge with hot wax prior to mounting it into the clamp's groove.

The main result of the test is the force versus elongation curve, from which strength and stiffness can be assessed. Since the thickness of the mesh is small and difficult to define and measure, due to its large pores, instead of using stress to generalize the results, we used force per unit width, as recommended by ASTM Standard D4595-11.

3. Results

Tensile tests performed along the longitudinal direction produced very different results from the ones performed along the transverse direction. Fig. 5 shows a sequence of photos taken at different load levels to a specimen being tested along the longitudinal direction. It is apparent that the rupture point is reached with moderate elongation as well as small reduction of the width (third photo from the left). Once this point is reached, the force starts to decrease because there are less filaments contributing to the strength of the mesh since some of them are broken.

Fig. 6 shows a similar test, but performed along the transverse direction. In this case, a quite large elongation is obtained without any filament being broken. The breaking point, where the maximum force is obtained, in this case was reached close to the limit of extension of the testing machine and is not shown in Fig. 6 because it will greatly enlarge the height of the figure. Altogether with the large elongation, an important reduction of the width can be observed, especially at the center of the specimen. This is produced by the action of the non-continuous, transverse filaments that in this test are oriented in the direction of the displacement of the clamps (vertical direction), on the longitudinal ones to which they are knotted to. Due to this particular knitting pattern, the straight, continuous longitudinal filaments (horizontal in this test) are forced to take a zigzag shape being pulled by the transverse, discontinuous filaments.

The force per unit width and elongation are the characteristics that are necessary to calculate the maximum wind that may resist the mesh of a LFC. The relationship between these two variables is shown in Fig. 7. It is seen that this mesh has an essentially linear (Hookean) behavior in the longitudinal direction, which is typical of elastic materials. This is a desired behavior for structural materials because it implies little permanent deformation, which means that the unloaded material recovers most of its initial dimensions. In contrast, in the transverse direction the behavior is non-linear, showing large elongations with small forces. This non-linear behavior is accompanied by permanent deformation of the mesh, which means that once it is stretched in this direction, will never recover its initial dimensions. Recalling that the stiffness is the slope of the force vs. elongation curve, results also show that the stiffness of the mesh is significant in the longitudinal direction (labeled E′ in Fig. 7), but is negligible (virtually zero)

[1] http://www.marienberg.cl/sobre-marienberg/.

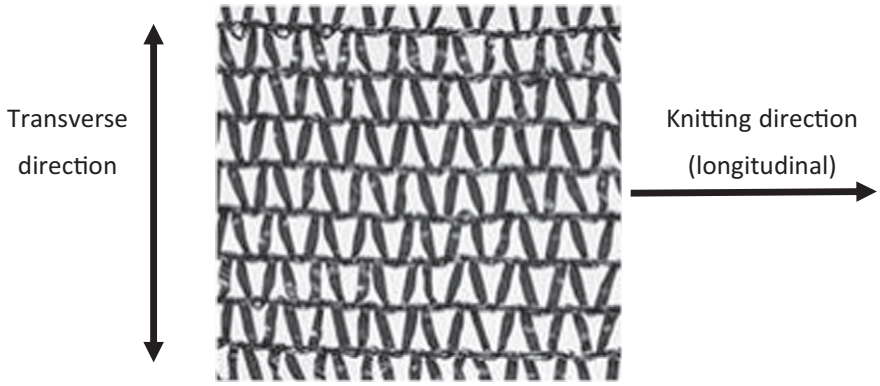

Fig. 2. Knitting pattern of the Raschel mesh used in the tests.

in the transverse direction at low deformation levels. In the longitudinal direction, breakage occurs at a 20% elongation, and the strength is more than 3.5 times the strength in the transverse direction.

4. Wind forces on LFCs

The test results described in the former section confirm that the Raschel mesh is indeed very anisotropic. In particular, it has significant strength and stiffness in the longitudinal direction, but has virtually no stiffness (non-negligible only at very large deformations) and a much lesser strength in the transverse direction. These characteristics are very important because they indicate that, when subjected to wind loads, a flat (i.e., bidirectional) Raschel mesh essentially works in a unidirectional manner, i.e., tensile forces act on the mesh only along the longitudinal direction.

Since the mesh cannot take bending moments, all the internal forces remain in the plane of the mesh. Therefore, even though the mesh under the effects of the wind takes a

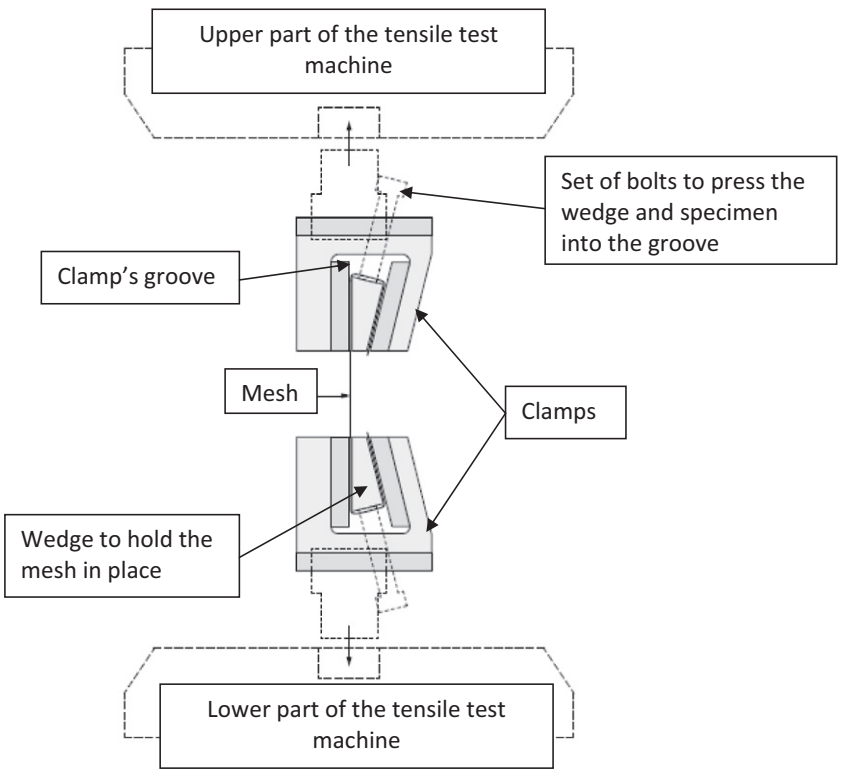

Fig. 3. Clamps for holding the mesh specimen in the tensile test machine. The wedge is pressed into the groove by a set of bolts and by the force applied to the mesh.

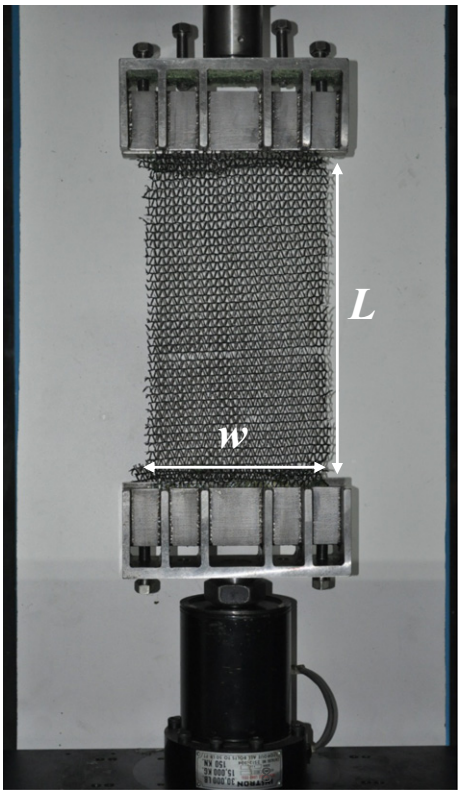

Fig. 4. Clamps and specimen mounted in the tensile test machine. This particular specimen is mounted with the transverse knitting direction oriented along the loading direction (vertical).

three-dimensional shape, the stress analysis is two-dimensional (basic plate theory, see for instance Park and Gamble, 2000). Considering the high anisotropy of the mesh, it is then possible to conclude that the maximum wind load that a LFC can withstand may be assessed by a relatively simple 2D model having strength and stiffness equal to those of the Raschel mesh in the longitudinal direction. Neglecting the contribution of the transverse direction introduces insignificant errors. Indeed, since the elongations are similar along both directions (Park and Gamble, 2000), the load taken by the transverse direction is extremely small at the elongation level where breakage occurs along the longitudinal direction (20%, Fig. 7).

Forces on LFCs subjected to wind loads are then assessed with the help of the 2D model schematically depicted in Fig. 8. The model assumes that the frame into which the mesh is attached is perfectly rigid and, therefore, does not deform when subjected to strong winds. The wind pressure stretches the mesh, which takes a bow shape. The total force of the wind acting on the mesh per unit width, F_w, is equal to the pressure difference across the mesh, Δp, times the projected mesh area, A, and it is balanced by the horizontal force on each side of the frame (Fig. 8), F_h.

$$F_w = \Delta p \cdot A = 2F_h \tag{1}$$

Since the mesh is a structural membrane, it does not take bending moments and, therefore, the only force it supports at the point of attachment to the rigid frame, F_t, is tangent to its surface, as shown in Figs. 8 and 9. Assuming the bow is approximately a circular section, which will indeed be if the pressure on the mesh is uniform, we can find a relationship between the tangential force F_t and the horizontal force F_h, which allows estimating the wind velocity that will break the mesh. The relationship between the tangential and horizontal forces is (Fig. 9)

$$F_h = F_t \sin\theta. \tag{2}$$

Since the frame is assumed as perfectly rigid, the radius R of the bow formed by the mesh and the angle θ depend only on mesh initial length and elongation, which are functions of the tangential force and the mesh modulus of elasticity. Indeed, the stretched length of the mesh, $L + \Delta L$, equals the

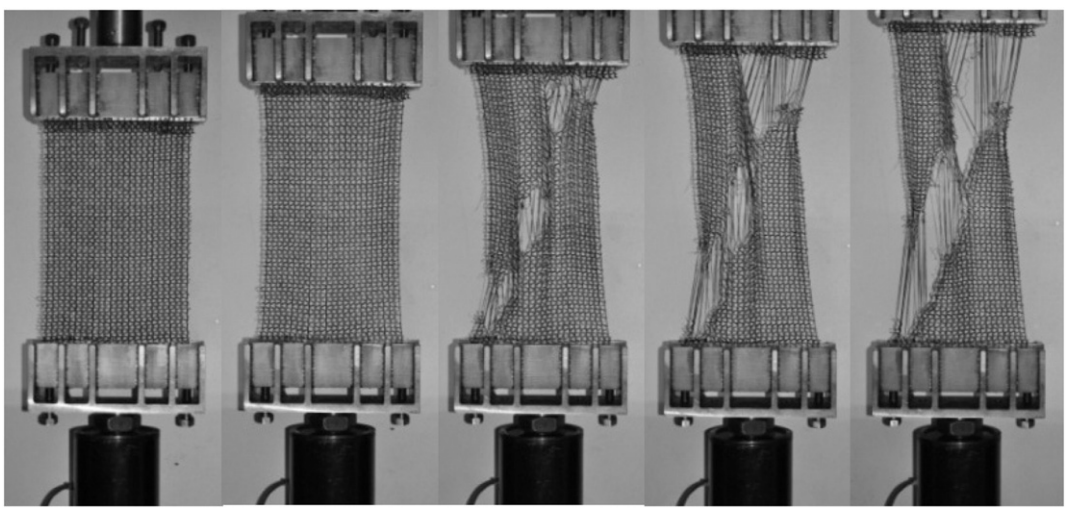

Fig. 5. Tensile test of Raschel mesh with 35% shade coefficient along the longitudinal direction. Maximum force is reached in the third photo from the left.

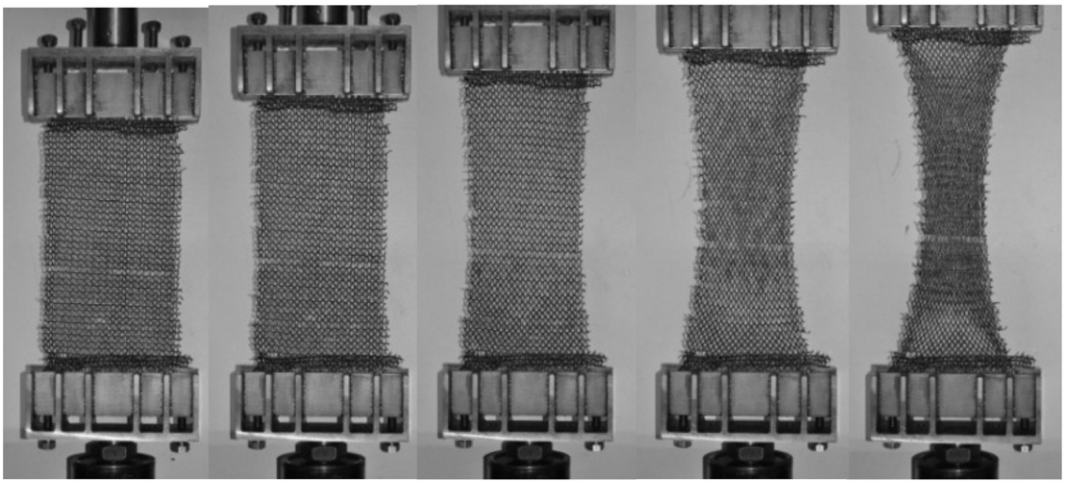

Fig. 6. Tensile test of Raschel mesh with 35% shade coefficient along the transverse direction. Maximum force is reached at a much larger elongation than the one corresponding to the last photo.

total angle of the circular bow, 2θ, times the radius R, and by definition of sine θ, we obtain Eqs. (3) and (4) that multiplied give Eq. (5).

$$2\theta \cdot R = L + \Delta L \tag{3}$$

$$\frac{L/2}{R} = \sin\theta \tag{4}$$

$$\frac{\theta}{\sin\theta} = 1 + \frac{\Delta L}{L} \tag{5}$$

Eq. (5) allows determining θ and sin θ given the mesh stretching. If the rupture force per unit width of the mesh, $F_{t_{rupt}}$, and its elongation at that point are known, we can calculate the wind pressure that will break the mesh by combining Eqs. (1) and (2), and calculating sin θ_{rupt} with Eq. (5). This approach leads to:

$$\Delta p_{\max} = \frac{2F_{t_{rupt}} \sin\theta_{rupt}}{L}. \tag{6}$$

Finally, we need to relate the pressure on the mesh with wind velocity. Holmes et al. (2014) made a thorough analysis of the effects of strong winds on LFCs, summarizing models for estimating wind pressure on the mesh as a function of wind velocity. They reviewed several publications on wind force over screens, both porous and impermeable (Richards and Robinson, 1999; Letchford et al., 2000; Letchford, 2001; Uematsu et al., 2008; Giannoulis et al., 2012) that agree in the general equations, but there are still disagreement on some details because of lack of sufficient experimental data. Nevertheless, there is agreement in the expression to determine wind pressure on a porous screen given by Eq. (7) (Richards and Robinson, 1999; Giannoulis et al., 2012), where s is the shade coefficient of the mesh, C_D is the drag coefficient of an impermeable screen of the same dimensions as the mesh, ρ is air density and v is wind velocity.

$$\Delta p = sC_D\rho\frac{v^2}{2} \tag{7}$$

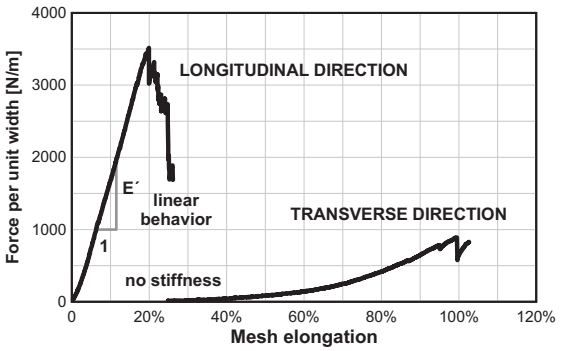

Fig. 7. Force per unit width vs. elongation of Raschel mesh, 35% shade coefficient.

The procedure to obtain the maximum wind velocity that the mesh of a particular LFC can withstand starts with obtaining the maximum force per unit width and corresponding elongation from tensile tests. With these values, calculate sin θ_{rupt} at this point using Eq. (5), Δp_{max} using Eq. (6) and, finally, the maximum wind velocity can be obtained from Eq. (7). Notice that Δp_{max} is inversely proportional to the distance L between the sides of the rigid frame.

With the results presented in Section 3 and the last two equations we can estimate the maximum wind velocity that this mesh can withstand in a typical LFC. Eq. (6) shows that the maximum wind pressure the mesh can withstand is inversely proportional to the distance between the sides of the frame to which the mesh is attached. This means that the smaller the size of the frame, the stronger the winds the mesh will take. Therefore, it is interesting to plot maximum wind speed versus frame dimension, which is presented in Fig. 10. This plot was made considering two layers of the tested Raschel mesh, because this is the way in which it is usually installed. Since the elongation is essentially the same

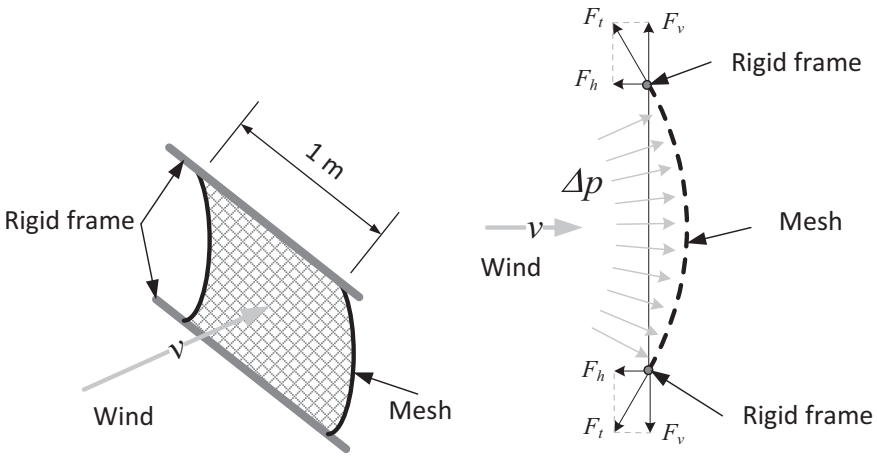

Fig. 8. Two-dimensional model of the forces acting on a mesh attached to a rigid frame.

in both layers, the total strength is simply twice the strength of a single layer. However, the uncertainty in the estimation of the wind force F_w is larger than for a single layer due to the unknown shade coefficient of the double mesh. A direct conclusion from the plot is that, from a structural point of view, Raschel meshes should be installed with the longitudinal direction aligned with the shortest dimension of the frame. This means that for a typical rectangular LFC where the vertical dimension of the frame is of the order of 4 m and the horizontal dimension is of the order of 10 m, the mesh should be installed with the longitudinal direction vertical if maximum strength and minimum deformation is desired. Nevertheless, from Fig. 10 it is clear that even if the mesh is installed with the longitudinal direction horizontally it will withstand very strong winds, over 50 m/s, an extremely rare event, but with larger deformation. Therefore, other practical considerations, apart from strength, may dictate the orientation of the mesh.

Eqs. (5) and (6) were derived assuming that the mesh is attached to a rigid frame, but in actual LFCs the mesh is in most cases attached to cables, which cannot be considered rigid but flexible because, when subjected to wind loads, they take a shape that departs considerably from the straight line of a rigid frame. The influence of the frame flexibility on the strength of LFCs can be deduced from the analysis of the mesh cross-section shown in Fig. 11. When subjected to winds, both ends of a mesh attached to a flexible frame move inwards and in the direction of the wind, increasing the angle θ. Since the tensile force $F_{t_{rupt}}$ at breakage is the same (it is an intrinsic property of the mesh), the value of $sin\ \theta$ increases, and so does the wind velocity at mesh breakage (Eqs. 6 and 7). In other words, the actual strength of a mesh attached to a flexible frame is somewhat greater than that of a rigid frame, but at the expense of more deformations.

5. Discussion

Fig. 10 shows that the Raschel mesh considered in this study, even when installed in quite large frames, can withstand

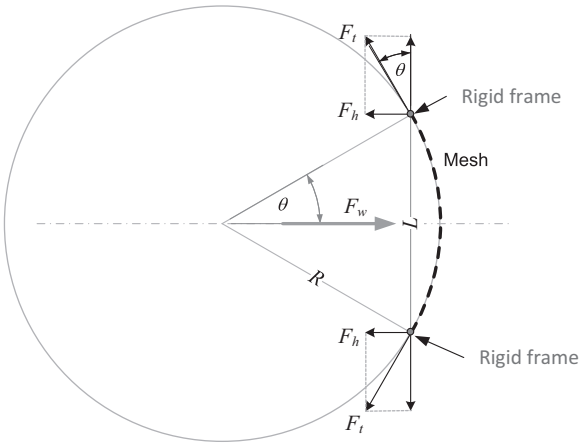

Fig. 9. Force decomposition assuming that the bow is a circular section of radius *R*.

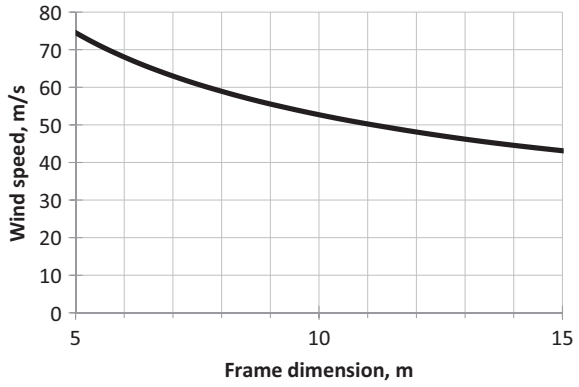

Fig. 10. Maximum wind speed that will withstand two layers of Raschel mesh with 35% shade coefficient. The frame dimension corresponds to the length of the mesh in the longitudinal direction, with no regards to whether its orientation is horizontal of vertical. Calculations were made with $C_D = 1.5$, $\rho = 1.15$, and the effective shade coefficient for the double layer is taken as 50% (Schemenauer and Joe, 1989).

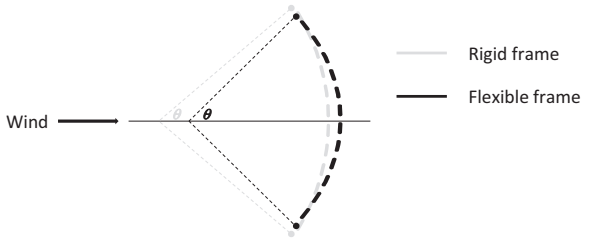

Fig. 11. Lateral view of a LFC: rigid frame vs. flexible frame.

very strong winds. Clearly, such winds impose severe loads on the members of the supporting structure. Since, as mentioned before, such members are usually not designed in accordance to structural engineering principles, it is then not surprising that many LFCs collapse because of either failure of the supporting structure or failure of the foundation. The mechanical properties of a typical Raschel mesh that are presented in this study can be used in structural analysis models of LFCs with which forces on the supporting structure can be rationally assessed, and its members (e.g., posts and cables) can then be rationally designed to withstand such forces.

However, as mentioned in Section 1, Introduction, some LFCs do not collapse but lose functionality because the mesh breaks. Since the wind velocities indicated in Fig. 10 are extremely rare in places where LFCs are usually installed, it is clear that in these instances the strength of the mesh turned out to be less than that determined in this study. In our opinion, there are at least two reasons why the actual strength of a Raschel mesh might be less than that determined in lab tests:

(a) The first reason is related to practical installation issues and is well known by people with practice in LFC installation. Indeed, as discussed in Holmes et al. (2014), the strength of the mesh might decrease considerably because of: (1) rubbing against other objects, which abrades the mesh filaments quite fast due to the almost permanent movement induced by wind and the poor wear resistance of polyethylene; (2) stress concentration in certain areas where the mesh is attached to the frame; and (3) weak spots created during installation as the mesh may be caught in sharp or pointed objects (e.g., small branches of surrounding bushes) and some filaments are broken. These observations clearly indicate that the correct erection of Raschel mesh in LFCs is very important and deserves serious consideration.

(b) The second reason is related to wind flow behavior and has not been mentioned previously in the literature. Wind flow has normally large scale turbulence that manifests as wind gusts. The forces induced on LFCs by wind gusts are dynamic with far more detrimental effects on structural elements. Additionally, wind gust speeds are of the order of 1.5 times the average wind speed registered by meteorological stations (Walshaw and Anderson, 2000). More on wind flow characteristics and wind gusts can be found in Briassoulis et al. (2010), Agustsson and Olafsson (2009), Boettcher et al. (2003), and Weggel (1999). The wind fluctuating velocity also produces cyclic forces that might contribute to unexpected breakage of the mesh. Moreover, vortex shedding also produces fluctuating pressures that contribute to cyclic loads. Clearly, standard tensile tests (monotonic load) cannot predict directly the behavior of the Raschel mesh subjected to both dynamic and cyclic loads. A theory and, probably, new tests, are then required.

6. Conclusions

Raschel mesh has a very anisotropic mechanical behavior, being much stronger and stiffer in the longitudinal (knitting) direction. Also stretching in this direction is elastic and elongation is far smaller than in the transverse direction. Based on these findings, it was determined that a flat mesh of a LFC behaves in an essentially unidirectional manner (i.e., tensile forces act only along the longitudinal direction) when subjected to wind loads. A relatively simple 2D model was then developed to assess the maximum wind load that a Raschel mesh can withstand. It was found that a Raschel mesh shall be installed with the longitudinal direction aligned with the shortest dimension of the frame if maximum strength and minimum deformation is desired.

It was also found that the Raschel mesh considered in this study should withstand extremely strong winds without damage. Therefore, mesh breakages commonly observed are most likely caused by factors that are known to reduce the strength of the mesh, such as stress concentration, rubbing with other objects, and weak spots produced during erection. The intrinsically dynamic nature of wind loads as a consequence of velocity fluctuation and vortex shedding is, in the long term, likely to induce breakage at wind velocities that are far less than those obtained considering the results of standard lab tests. This phenomenon has not been studied in detail and is certainly recommended for future research.

Acknowledgments

The authors want to acknowledge the grant from Vicerrectoria de Investigacion of Pontificia Universidad Catolica de Chile, Grant no. 2641-121-81. They also wish to acknowledge Mr. Javier Ramos, graduate student at MIT, for performing the tensile tests and processing the data, and Mr. Patricio Perez from the Lab of Metallurgy, Pontificia Universidad Catolica de Chile, for helping with the operation of the testing machine.

References

Abdul-Wahab, S.A., Lea, V., 2008. Reviewing fog water collection worldwide and in Oman. Int. J. Environ. Stud. 65, 485–498.
Abdul-Wahab, S.A., Al-Damkhi, A.M., Al-Hinai, H., Al-Najar, K.A., Al-Kalbani, M.S., 2010. Total fog and rainwater collection in the Dhofar region of the Sultanate of Oman during the monsoon season. Water Int. 35, 100–109.
Agustsson, H., Olafsson, H., 2009. Forecasting wind gusts in complex terrain. Meteorog. Atmos. Phys. 103, 173–185. http://dx.doi.org/10.1007/s00703-008-0347-y.
Al-hassan, G.A., 2009. Fog Water Collection Evaluation in Asir Region–Saudi Arabia. Water Resour. Manag. 23, 2805–2813. http://dx.doi.org/10.1007/s11269-009-9410-9.
Boettcher, F., Renner, Ch., Waldl, H.P., Peinke, J., 2003. On the statistics of wind gusts, Boundary-Layer. Meteorology 108, 163–173.
Briassoulis, D., Mistriotis, A., Giannoulis, A., 2010. Wind forces on porous elevated panels. J. Wind Eng. Ind. Aerodyn. 98, 919–928.

Cereceda, P., Osses, P., Larrain, H., Farías, M., Lagos, M., Pinto, R., Schemenauer, R.S., 2002. Advective, orographic and radiation fog in the Tarapacá region. Chile Atmos. Res. 64, 261–271.
Cereceda, P., Larrain, H., Osses, P., Farías, M., Egaña, I., 2008a. The climate of the coast and fog zone in the Tarapacá Region, Atacama Desert. Chile Atmos. Res. 87, 301–311.
Cereceda, P., Larrain, H., Osses, P., Farías, M., Egaña, I., 2008b. The spatial and temporal variability of fog and its relation to fog oasis in the Atacama Desert. Chile. Atmos. Res. 87, 312–323.
de la Lastra, C., 2002. Report on the Fog-collecting Project in Chungungo: Assessment of the Feasibility of Assuring its Sustainability. International Development Research Centre (IDRC), Ottawa, Ont, Canada (online).
Estrela, M.J., Valiente, J.A., Corell, D., Millán, M.M., 2008. Fog collection in the western Mediterranean basin (Valencia region, Spain). Atmos. Res. 87, 324–337.
Gandhidasan, P., Abualhamayel, H.I., 2007. Fog collection as a source of fresh water supply in the Kingdom of Saudi Arabia. Water Environ. J. 21, 19–25. http://dx.doi.org/10.1111/j.1747-6593.2006.00041.x.
Giannouilis, A., Stathopoulos, T., Briassoulis, D., Mistriotis, A., 2012. Wind loading on vertical panels with different permeabilities. J. Wind Eng. Ind. Aerodyn. 107–108, 1–16.
Gischler, C., 1991. The missing link in a production chain, vertical obstacles to catch Camanchaca. ROSTLAC-UNESCO, Montevideo — Uruguay. http://unesdoc.unesco.org/Ulis/cgi-bin/ulis.pl?database=&lin=1&futf8=1&ll=c&gp=&look=default&sc1=1&sc2=1&ref=https://www.google.cl/&nl=1&req=2&text=IDRC%20Camanchaca%20Project%20(Chile)&text_p=phrase+like (ISBN 92-9089-019-7. Available as pdf document at).
Holmes, R., Rivera, J.D., de la Jara, E., 2014. Large fog collectors: New strategies for collection efficiency and structural response to wind pressure. Atmos. Res 151, 236–249.
Klemm, O., Schemenauer, R.S., Lummerich, A., Cereceda, P., Marzol, V., Corell, D., van Heerden, J., Reinhard, D., Gherezghiher, T., Olivier, J., Osses, P., Sarsour, J., Frost, E., Estrela, M.J., Valiente, J.A., Fessehaye, G.M., 2012. Fog as a fresh-water resource: overview and perspectives. AMBIO. http://dx.doi.org/10.1007/s13280-012-0247-8.
Larrain, H., Velásquez, P., Cereceda, P., Espejo, R., Pinto, R., Osses, P., Schemenauer, R.S., 2002. Fog measurements at the site "Falda Verde" north of Chañaral compared with other fog stations of Chile. Atmos. Res. 64, 273–284.
Letchford, C., 2001. Wind loads on rectangular signboards and hoardings. J. Wind Eng. Ind. Aerodyn. 89 (2), 135–151 (Available at: http://linkinghub.elsevier.com/retrieve/pii/S0167610500000684).
Letchford, C.W., et al., 2000. Mean wind loads on porous canopy roofs. J. Wind Eng. Ind. Aerodyn. 84 (2), 197–213 (Available at: http://linkinghub.elsevier.com/retrieve/pii/S0167610599001038).
Louw, C., van Heerden, J., Olivier, J., 1998. The South African fog-water collection experiment: meteorological features associated with water collection along the eastern escarpment of South Africa. Water SA 24, 269–280.
Lummerich, A., Tiedemann, K.J., 2011. Fog water harvesting on the verge of economic competitiveness. ERKUNDE 65 (3), 305–306.
Marzol, M.V., 2002. Fog water collection in a rural park in the Canary Islands (Spain). Atmos. Res. 64, 239–250.
Marzol, M.V., 2008. Temporal characteristics and fog water collection during summer in Tenerife (Canary Islands, Spain). Atmos. Res. 87, 352–361.
Marzol, M.V., Sánchez, J.L., 2008. Fog water harvesting in Ifni, Morocco. An assessment of potential and demand. Erde 139, 97–119.
Olivier, J., 2002. Fog-water harvesting along the West Coast of South Africa: a feasibility study. Water SA 28, 349–360.
Olivier, J., de Rautenbach, C.J., 2002. The implementation of fog water collection systems in South Africa. Atmos. Res. 64, 227–238.
Park, R., Gamble, W.L., 2000. Reinforced Concrete Slabs, 2nd edition. Wiley, New York, USA.
Richards, P., Robinson, M., 1999. Wind loads on porous structures. J. Wind Eng. Ind. Aerodyn. 83 (1–3), 455–465.
Schemenauer, R.S., Cereceda, P., 1991. Fog-water collection in arid coastal locations. AMBIO 20, 303–308.
Schemenauer, R.S., Cereceda, P., 1994. The role of wind in rainwater catchment and fog collection. Water Int. 19, 70–76.
Schemenauer, R.S., Joe, P.I., 1989. The collection efficiency of a massive fog collector. Atmos. Res. 24, 53–69.
Schemenauer, R.S., Fuenzalida, H., Cereceda, P., 1988. A neglected water resource: the Camanchaca of South America. Bull. Am. Meteorol. Soc. 69, 138–147.
Schemenauer, R.S., Cereceda, P., Osses, P., 2005. Fog water collection manual. FogQuest, Ontario, Canada. www.fogquest.org (2005).
Shanyengana, E.S., Henschel, J.R., Seely, M.K., Sanderson, R.D., 2002. Exploring fog as a supplementary water source in Namibia. Atmos. Res. 64, 251–259.
Uematsu, Y., Stathopoulos, T., Iizumi, E., 2008. Wind loads on free-standing canopy roofs: part 1 local wind pressures. J. Wind Eng. Ind. Aerodyn. 96 (6–7), 1015–1028 (Available at: http://linkinghub.elsevier.com/retrieve/pii/S016761050700150X. [Accessed April 29, 2013]).
Walshaw, D., Anderson, C.W., 2000. A model for extreme wind gusts. Appl. Stat. 49, 499–508 (Part 4).
Weggel, J.R., 1999. Maximum daily wind gusts related to mean daily wind speed. J. Struct. Eng. 125, 465–468.